

Structural and Functional Impacts of the Altered Hydrophobicity in the Dimer Interface of *Tpv* HSP 14.3

Sema ZABCI^{1*}, Azra RAFIQ², Semra KOCABIYIK¹

¹Middle East Technical University, Faculty of Art and Science, Department of Biological Sciences, 06800, Ankara, Türkiye

²Riphah International University, Faculty of Pharmacy, Department of Pharmaceutical Sciences, 54000, Lahore, Pakistan

ABSTRACT: Small heat shock proteins (sHSPs) are the ATP-independent molecular chaperones that prevent protein aggregation in the cell by forming stable complexes with unfolded and misfolded proteins. Their distinctive structural characteristics are their low molecular weight (from 14 to 43 kDa) and a tripartite domain architecture. The highly conserved Alpha Crystallin Domain (ACD) plays a central role in the dimerization of sHSPs and acts as the structural building block for oligomerization. The point mutations in the ACD of the human sHSPs that interfere with the dimer integrity are linked to several diseases, including cataracts, desmin-related myopathy, cardiomyopathy, and distal hereditary motor neuropathy. In the present study, we investigated the functional and structural implications of amino acid changes at two putative dimer interface residues, L33 and Y34. These residues are located on the $\beta 2$ strand of *Tpv* HSP 14.3, which is implicated in ACD dimerization via strand exchange. Effects of the substitutions were evaluated by performing chaperone assays using the client proteins pig heart Citrate Synthase (phCS) and Alcohol Dehydrogenase (ADH) and through *in silico* molecular bond and structure analyses of the wild type and generated mutant proteins. Our results indicated that an excess amount of WT and the mutant proteins are required to maintain phCS activity to a level comparable to or even higher than the positive control. At a lower substrate/sHSP ratio, the Y34F mutant protected the phCS activity more effectively than the WT and L33S mutant sHSPs. Also, the Y34F mutant sHSP afforded the highest protection of ADH enzyme from heat inactivation. It is likely that increased hydrophobicity by Y34F substitution contributed to the formation of a hydrophobic surface that may capture aggregation-prone substrates. According to molecular bond analysis, the loss of intermolecular hydrophobic interactions between leucine 33 on the $\beta 2$ strand and tyrosine 77 and isoleucine 78 on the $\beta 6$ strand can be critical for the reduced structural/thermodynamic stability of the L33S mutant protein.

Keywords: *Thermoplasma volcanium*, small heat shock protein (sHSP), site-directed mutagenesis, dimer interface, alpha crystallin domain, 3-D structure analysis.

*Corresponding Author: Sema ZABCI
E-mail: sema.zabc@yahoo.com
Submitted: 23.11.2023 Accepted: 02.12.2023

1 INTRODUCTION

Small heat shock proteins (sHSPs) are the ATP-independent molecular chaperones that play essential roles in maintaining protein homeostasis in the cells [1]. The sHSPs are constitutively expressed to prevent protein aggregation, and their expression level is immediately induced upon exposure to stress factors (*e.g.*, heat, oxidative, and pH stress) [2]. They form stable complexes with denaturing proteins and sequester them in a folding-competent state. Substrate release and subsequent refolding are achieved through the participation of ATP-dependent chaperones such as Hsp70 and Hsp100 [3]. The sHSPs are present in three kingdoms of life and some viruses. The low molecular weight (*i.e.*, 12 to 43 kDa) and a tripartite domain architecture are their characteristic structural features [4]. The unique central element α -crystallin domain (ACD) is highly conserved and composed of seven to eight β -sheets that adopt an immunoglobulin fold. The ACD (consists of 90–100 amino acids) is flanked by variable and flexible N-terminal domain (NTD) and C-terminal domain (CTD) [5]. The ACD plays an important role in the dimerization of sHSP, and the ACD dimer is the basic building unit for the subsequent oligomerization of small heat shock

proteins [6, 7]. There are two types of defined dimerization modes. In non-metazoans (archaeal, bacterial, yeast, and plant), a symmetric dimer is formed by strand exchange in the ACD of sHSPs so that the β_6 strand of one ACD interacts with the β_2 strand of the partnering ACD. In metazoan sHSPs, the extended β_6 - β_7 strands of the partnering ACDs are linked through ionic and hydrophobic interactions and hydrogen bonds, leading to the formation of the ACD dimer [8, 9]. Starting from the ACD dimer, the formation of higher-order oligomers (12 to > 48 subunits) involves a hierarchy of interactions by the participation of NTE and CTE elements [10, 11]. The highly polydisperse oligomeric forms of sHSPs are dynamic and can dissociate into smaller species, predominantly dimers, as a response to changes in conditions such as temperature and pH or modifications such as phosphorylation. This dynamic feature is crucial for the chaperone function of sHSPs [12].

The interaction between the two sheets of the ACD dimer is relatively weak, with a dissociation constant in the order of a few micromolar [13]. There are several reports indicating that disruption of the dimer interface in human sHSPs by mutations, which are diseases associated, had significant effects on the structure and

function of the sHSPs by blocking subunit exchange [14]. Among such mutations, there are cataract associated R116C mutation of α A-crystallin, desmin related myopathy and cardiomyopathy associated R120G mutation of α B-crystallin, and distal hereditary motor neuropathy related K141E mutation of HSP22 [14–18]. The equivalent of these residues is arginine 107 in the archaea *Methanocaldococcus jannaschii* (Mj) Hsp 16.5, and the R107G substitution resulted in the formation of larger and more polydisperse oligomers than the wild type MjHsp16.5 [19]. Except this, there is not any report on the investigation of the dimer interface interactions by targeting specific residues in archaeal sHSPs.

In this study, we aimed to fill the gaps in the literature concerning the role of hydrophobicity in the dimer interface of sHSPs. In our experiments, we specifically targeted two residues, L33 and Y34, of the *Tpv* HSP 14.3, which are predicted as putative interface residues by the NCBI Conserved Domain Database search. These residues are located on the β 2 strand, which is directly involved in dimerization by interconnecting with the β 6 loop. The hydrophobicity of the dimer interface was altered by site-specific mutagenesis. Chaperone activity assays and *in silico* molecular bond and structure analyses of the wild type and mutant proteins were

performed in comparison with the wild types.

2 MATERIAL AND METHOD

2.1 Recombinant Plasmid Construction

The recombinant *Tpv* HSP 14.3 gene encoding Hsp20/alpha crystallin family protein (locus name TVG_RS04180, sequences 790978..791352) of *Thermoplasma volcanium* [20] was cloned into the expression vector pET21a (+) (Novagen, Madison, WI) following the Kit protocol. The *Tpv* HSP 14.3 gene from the plasmid pDrive-tpv14.3 was amplified by PCR (Gene Cyclor, Techne Inc., NJ, USA) using the forward primer (5'-TGAGCATATGTATACACCCATAAAGTTCTTTACG-3') with *Nde*I recognition site and the reverse primer (5'-TGAGGGATCCCACCCAATCACATCAAGCATAAC-3') with *Bam*HI recognition site. After purification (QIAquick Gel Extraction Kit, QIAGEN Inc., Valencia, USA), the amplified gene was introduced into the expression vector pET21a (+) at *Nde*I and *Bam*HI sites using DNA Ligation Kit (Novagen, Madison, WI). Putative recombinant plasmids were transferred into chemically competent *E.coli* BL21 (DE3) cells (New England Biolabs, Ipswich, Massachusetts) by transformation. The sequences of the plasmids from selected

recombinant clones were confirmed by DNA sequencing (Oligomer Company, Ankara, Türkiye). One of the verified expression constructs carrying the *Tpv* HSP 14.3 gene was named pET21_tvshSP2 and transformed into *E.coli* BL21 (DE3) cells (New England Biolabs, Ipswich, Massachusetts) for expression of the wild type sHSP.

2.2 Site-Directed Mutagenesis

Single amino acid substitution (L33S and Y34F) mutants of the *Tpv* HSP 14.3 were generated by PCR-mediated mutagenesis using Quick-Change II Site-Directed Mutagenesis Kit (Agilent Technologies Inc. Santa Clara, California, USA). The mutagenic oligonucleotide primer pairs that were designed according to Kit's instructions are given in Table 1. The recombinant plasmid pET21_tvshSP2 with cloned *Tpv* HSP 14.3 gene was used as the template in the mutagenesis experiments. The mutations were verified by DNA sequencing (Genscript Biotech, Piscataway, New Jersey, USA). For high efficiency protein expression, mutant plasmid constructs were transformed into competent *Escherichia coli* BL21(DE3) cells.

Table 1. List of the mutagenic oligonucleotide forward (f) and reverse (r) primers

Mutation	Sequence of the Mutagenic Oligonucleotide Primers
L33S-f	5'-cca ccagtcacgtca tat caa gat agc-3'
L33S-r	5'-ctatcttgatatgacgtgactggtgg-3'
Y34F-f	5'-cca ccagtcacgttatttcaa gat agc tct-3'
Y34F-r	5'-agagctatcttgaataacgtgactggtgg-3'

2.3 Protein Expression and Purification

The cell lysates were prepared mainly according to the pET System Manual Instructions. Overnight cultures of wild type and mutant *E.coli* BL21(DE3) strains were grown at 37°C in Luria-Bertani (LB) medium containing ampicillin (100 µg/mL) with vigorous shaking to an OD₆₀₀ of 0.5-0.7. Overexpression was induced by adding isopropyl thio-β-D-galactoside (IPTG) to a final concentration of 1 mM. The growth was continued for 4-5 hours before cells were harvested by centrifugation at 5000 x g for 20 min at 4°C (JOUAN SA, Herblain-France). The cell pellet was resuspended in 10 mL lysis buffer (25 mM Tris, 1 mM EDTA, 30 mM NaCl pH 7.5). The cells were broken by sonication (Sonics and Materials, USA), and supernatants of the lysates were obtained by centrifugation at 20000 xg for 20 min at 4°C (Sigma 3K30 Centrifuge, Sigma Chemical Co., USA). The supernatant fraction containing soluble sHSP was heated between 60°C and 80°C

to investigate the expressed protein's heat stability. The denatured protein was removed by centrifugation at 12000 xg for 1 hour at 4°C. The cleared lysate was stored at -20°C until use.

SDS polyacrylamide gel electrophoresis (SDS-PAGE) was used to analyze the progress of the expression. For purification, the soluble protein fractions were applied to a pre-packed anion exchange HiTrap Q column (Amersham Biosciences, U.S.A.), connected to the AKTA prime HPLC system (Amersham Biosciences, U.S.A.). The bound proteins were eluted at a flow rate of 5.0 mL/min with a linear gradient of NaCl (0-1 M) in the start buffer (20 mM Tris, pH 8.41). Peak fractions containing *Tpv* HSP 14.3 as deduced by SDS-PAGE gel and OD280 measurements (Picopet 01, Picodrop Ltd. U.K.), were pooled, concentrated, and desalted by ultracentrifugation (Vivaspin 5 kDa cut-off, Sartorius, Germany). Purity was checked by SDS-PAGE.

2.4 Chaperone Activity Assays

Chaperone activities of the *Tpv* HSP 14.3 and mutant variants were characterized as the ability to protect the client proteins pig heart Citrate Synthase (phCS) (EC 4.1.3.7, Sigma) and Alcohol Dehydrogenase (ADH) (EC 1.1.1.1, Sigma) from heat-induced inactivation, as described previously [20, 21].

phCS heat protection assay was performed by pre-incubating the enzyme at 47°C for 10 min in the presence or absence of the sHSP. Then, the remaining CS activity was measured at 35°C by continuously monitoring the absorbance at 412 nm (Shimadzu UV-1601A, Kyoto, Japan). The protection effect of *Tpv* HSP 14.3 was evaluated at three substrate/sHSP, w/w ratios of 1:500, 1:250, and 1:147.

For the ADH heat protection assay, the enzyme was pre-heated at 47°C for 20 minutes, with or without *Tpv* HSP 14.3 protein at an ADH/chaperone (w/w) ratio of 1:90. The ADH activity was measured by continuously recording the rate of NAD⁺ reduction spectrophotometrically at 340 nm [21].

Each experiment was repeated at least three times. The data analysis and plotting of the graphics were achieved by using GraphPad Prism 9.0 software (GraphPad, USA).

2.5 Bioinformatics and 3-D Structure Analysis

The multiple alignments (MSA) were performed by the Clustal W Program in the EMBL-EBI database (<https://www.ebi.ac.uk/Tools/msa/clustalo/>). The secondary structure features incorporated into the MSA were obtained by the Jalview [22]. Putative dimer interface residues were predicted by Conserved Domain Database (CCD) search (National

Center for Biotechnology Information, <https://www.ncbi.nlm.nih.gov/cdd/>). The homology model of the *Tpv* HSP 14.3 3-D structure was generated by MODELLER 9.15 Ver server. Crystal structures of *Xanthomonas axonopodis* (PDB entry 3GLA), *Sulfolobus tokodaii* (PDB entry 3AAC and 3VQM), and *Deinococcus radiodurans* (PDB entry 4FEI) were used as templates. Visualization, energy minimization, and structure analyses of the models were achieved using the UCSF Chimera Program. The BIOVIA Discovery Studio Visualizer (DSV) (Ver 4.5) was used for the analysis of the weak molecular interactions in the generated 3-D models. Thermodynamic stability analysis of the *Tpv* HSP 14.3 proteins was performed using the MUpro web server [23].

3 RESULT

3.1 Multi-Sequence Alignment of ACD Sequences of *Tpv* HSP 14.3 and Other Representative Archaeal sHSPs

Multiple sequence alignment of the ACD sequences of the archaeal sHSPs showed that highly conserved residues were found in the core alpha-crystallin domain spanning residues L33-K114 in *Tpv* HSP 14.3. The similarity scores range from 52.7 % to 90.2 % within the total 82 amino acid ACD sequence. The ACD is composed of eight beta strands named from β 2 to β 9 (Figure 1). The residues we targeted for

mutagenesis, L33 and Y34, are predicted as two of the residues forming the monomer-monomer interface. These amino acids reside on the β 2 strand, which is involved in dimerization by interacting with the β 6 strand of the partner monomer. The equivalent residues at position 33 are all hydrophobic residues *i.e.*, methionine or isoleucine. This may indicate the importance of hydrophobicity at this position and its possible involvement in hydrophobic interaction in the dimer interface. The tyrosine at position 34 is also highly conserved, except the sHSPs of hyperthermophilic archaea, *Pyrococcus furious* and *Thermococcus kodakarensis*, where F exists at the corresponding position. The common feature of these amino acids is their aromatic side chains.

3.2 Heat Stability of *Tpv* HSP 14.3 Wild Type and ACD Mutants

Before and after heating, when the cell lysates of the wild type (WT) and mutant *Tpv* HSP 14.3 proteins were separated into soluble and insoluble (pellet) fractions by centrifugation and analyzed by SDS PAGE, a significant amount of all sHSPs was recovered in the soluble fraction (Figure 2, Lane1). However, the sHSP was absent in the cell lysate of the *E.coli* BL21(DE3) cells without *Tpv* HSP 14.3 plasmid (negative control), since the sHSP-specific band was not detected on the gel. These results

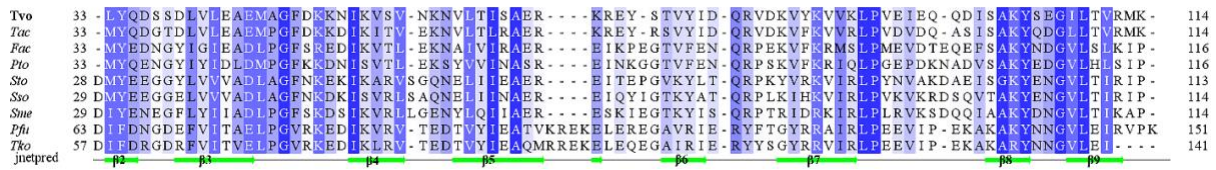


Figure 1. Multiple sequence alignment of alpha crystallin domain of *Tpv* HSP 14.3 with the sHSPs from other archaea. The species names and accession number of their sHSPs are: Tvo; *Thermoplasma volcanium* (CBY78065.1: GSS1), Tac; *Thermoplasma acidophilum* (CAC11993.1: DSM 1728), Fac; *Ferroplasma acidiphilum* (ARD84221.1: Y), Pto; *Picrophilus torridus* (AAT43324: DSM 9790), Sto; *Sulfurisphaera tokodaii* (WP_010979712.1: Str.7), Sso; *Saccharolobus solfataricus* (WP_009989320.1: P2), Sme; *Sulfuracidifex metallicus* (WP_054838418.1, DSM 6482), Pfu; *Pyrococcus furiosus* (AAF71367.1: DSM 3638), Tko; *Thermococcus kodakarensis* (WP_048053707.1: KOD1). Highly conserved residues are shaded by dark blue. Secondary structural features of the ACD are indicated below the alignment. The β strands from $\beta 2$ through $\beta 9$ are underlined by green arrows.

indicated the successful expression of recombinant WT and mutant proteins and the effectiveness of the IPTG induction for overexpression (Figure 2b). The L33S and Y34F substitutions produced mutant proteins, which are stable at temperatures up to 70°C (Figure 2b and 2c). Above this temperature (80°C), the sHSP bands, particularly that of the L33S protein, were hardly detectable in the cell lysates of the mutant proteins.

3.3 Functional Characterization of the *Tpv* HSP 14.3 WT and Mutant Proteins

To assess the chaperone functions of sHSP proteins, the WT and mutant proteins were

compared for their ability to protect the client proteins pHCS and ADH from denaturation during heating at 47°C as described in the Material and Methods.

Our results showed that when heated in the absence of sHSP, the pHCS activity decreased about 11-fold, so that only 8% of the activity could be recovered (Figure 3). Heat protection efficiency of the WT and mutant sHSPs appeared to be concentration dependent, increasing with increased substrate/sHSP w/w ratio. At a 1:147 CS/sHSP (w/w) ratio, all sHSP variants provided almost equal protection of the pHCS activity from heat inactivation. Only

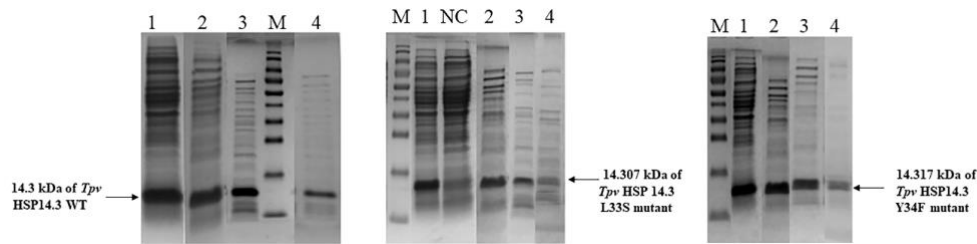


Figure 2. SDS PAGE analysis of wild type *Tpv* HSP 14.3 and its variants before and after heat treatment. a) WT *Tpv* HSP 14.3 b) L33S *Tpv* HSP 14.3 c) Y34F *Tpv* HSP 14.3 M: Page Ruler Pre-Stained Protein Ladder (SM0671, Fermentas). NC: Negative Control. Lane 1: Cell free extract of the *Tpv* HSP 14.3 before heat treatment (BH), Lane 2-4: Heat treatment at 60°C, 70°C, and 80°C, respectively.

~ 30% protection of CS activity could be supported at this substrate/sHSP ratio. At the 1:250 phCS/sHSP (w/w) ratio, the WT and L33S mutant sHSPs achieved ~50% protection of the CS enzyme activity, while Y34F supported relatively higher protection (~67%). At the 1:500 CS/ sHSP (w/w) ratio, the WT sHSP fully protected the CS activity. Remarkably, at the same substrate/sHSP ratio, L33S and Y34F mutants afforded a notable increase (additional 8 to 9 % protection) in the CS activity as compared to WT sHSP.

These results indicated that an excess amount of WT and the mutant proteins are required to maintain CS activity to a level comparable to or even higher than the PC. At lower substrate/sHSP ratio, Y34F sHSP protected the CS activity more effectively than the WT and L33S mutant sHSPs.



Figure 3. Effect of *Tpv* HSP 14.3 wild type and its mutants on the prevention of CS from thermal inactivation at different CS/sHSP ratios (w/w). After heating at 47°C for 10 min, the remaining activity was assessed by continuously monitoring absorbance at 412 nm. The initial rate of the reaction was calculated as the slope of the increase in absorption. PC: Positive Control, activity measured before heat treatment. NC: Negative Control, remaining activity after heat treatment without the presence of a chaperone. The presented data represent mean values with standard deviation (at the top of each bar) based on a minimum of three independent experiments.

To extend our investigation of the capacity of *Tpv* HSP 14.3 wild type and mutant variant proteins to protect the substrate proteins from heat, we have tested their chaperone activities against thermal inactivation of the ADH enzyme at a 1/90 substrate/ sHSP (w/w) ratio. The enzyme activity assay revealed that heating the enzyme at 47°C for 20 minutes in the absence of *Tpv* HSP 14.3 (negative control) resulted in a dramatic decrease (~95%) in the ADH activity (Figure 4). However, in the presence of *Tpv* HSP 14.3 WT, 64% of the ADH activity was recovered as compared to the negative control. The chaperone activities of the mutant sHSPs were better than the WT sHSP and about 75% and 87 % of the initial ADH activity was protected by L33S and Y34F mutant sHSP, respectively.

Thus, it is evident from our experiments that the Y34F mutant sHSP has a greater ability compared with other sHSP variants to protect the ADH and phCS from heat inactivation.

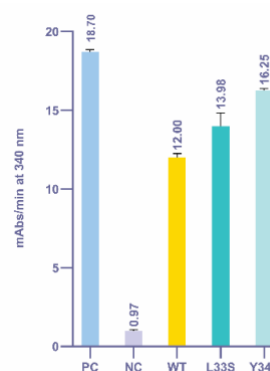


Figure 4. ADH activity assay in the absence and presence of *Tpv* HSP 14.3. The ADH was heated at 47°C for 20 min in the presence or absence of the chaperone. The rate of reduction of NAD^+ was measured at 340 nm. The rate of the reaction was found by analyzing the slope of the initial increase in absorption. PC: Positive Control, activity measured before heat treatment. NC: Negative Control, remaining activity after heat treatment without the presence of a chaperone. The presented data represent mean values with standard deviation (at the top of each bar) based on a minimum of three independent experiments.

3.4 3-D Structure Analysis of *Tpv* HSP 14.3 and its Molecular Interactions

The 3-D structure of *Thermoplasma volcanium* HSP 14.3 was generated by homology modelling. The ACD of *Tpv* HSP 14.3 is like an immunoglobulin fold consisting of two anti-parallel layers such that β_2 , β_3 , β_8 , β_9 form one layer and β_4 , β_5 , and β_7 together with a distinct β_6 for the other sheet. A large β_6 loop protrudes from

an additional β strand between $\beta 5$ and $\beta 7$, which is absent in the ACD of vertebrate sHSPs. This loop is positioned close to the $\beta 2$ strand of the adjacent monomer and directly involved in ACD dimer formation *via* strand exchange, which is typical for the non-metazoan sHSPs [6]. This core ACD is flanked by an N-terminal region that shows an α -helical structure and an unstructured C-terminal domain (Figure 5).

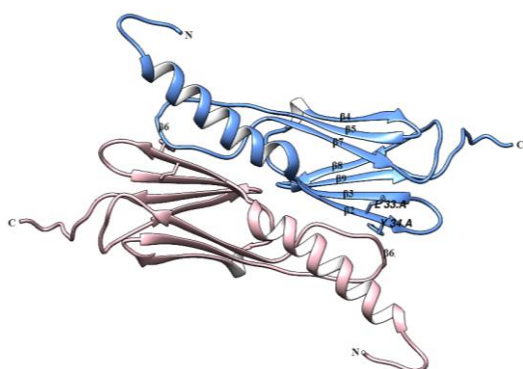


Figure 5. The model structure of *Tpv* HSP 14.3. Interacting monomers of the *Tpv* HSP 14.3 dimer are shown as ribbon diagrams (blue and pink). For clarity, strands $\beta 2$ to $\beta 9$ are labeled for only one monomer (colored blue). The L33 and Y34 residues are also indicated on the $\beta 2$ strand.

The changes in the hydrophobicity characteristics of the ACD dimer surface by amino acid substitutions could be recognized by molecular surface analysis of the 3-D model structures by the CHIMERA program. This program colors the molecular surface according to the hydrophobicity amino acid, ranging from Dodger Blue to red, representing the minimum and maximum values on the Kyte-Doolittle scale.

To understand how the introduced mutations affected the surface properties, 3-D hydrophobicity surface models of *Tpv* HSP 14.3 WT and the mutants were generated. The L33S mutation at this position changed color from red to blue, signifying a reduction in surface hydrophobicity by the introduction of the polar residue serine for the very hydrophobic leucine. On the other hand, the replacement of the tyrosine at position 34 with the highly hydrophobic amino acid phenylalanine enhanced surface hydrophobicity relative to the WT, which is evident from the blue-to-red transition at this position (Figure 6).

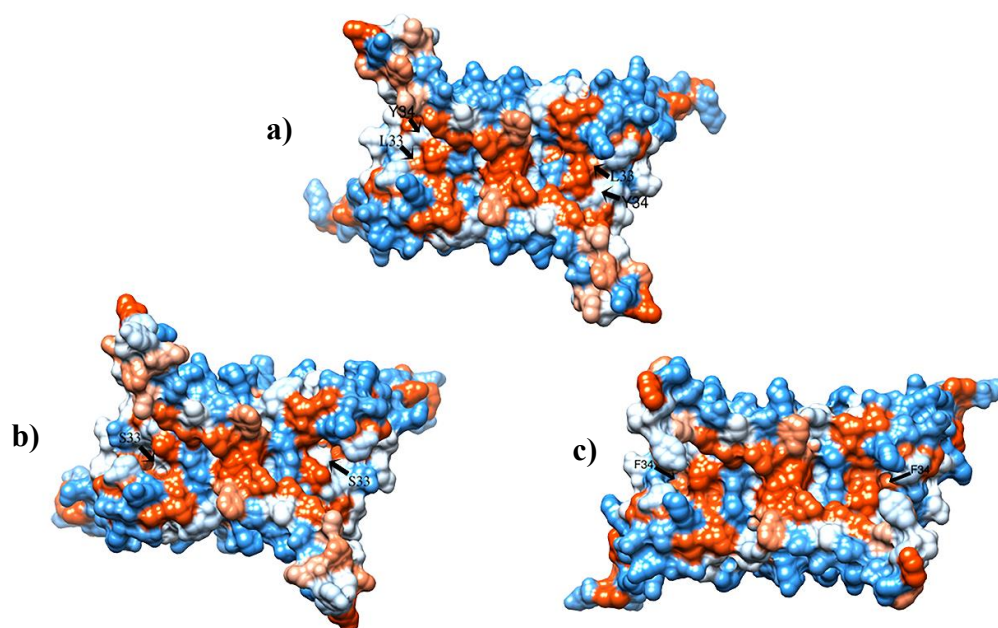


Figure 6. Surface hydrophobicity analysis of *Tpv* HSP 14.3 and its ACD mutants. a) *Tpv* HSP 14.3 WT, b) L33S mutant, c) Y34F mutant. The arrows show the locations of the targeted mutations in which surface hydrophobicity is changed relative to the WT. Min and max values are associated with bright blue and orange-red, respectively.

Comparative analysis of the intra/intermolecular bonds after point mutations was performed by the DSV Program. As a result of the replacement of the hydrophobic amino acid leucine with the polar amino acid serine at position 33 (L33S) resulted in the loss of intramolecular hydrophobic bonds of Leu33-Leu42 and the intermolecular hydrophobic bonds of Leu33-Ile78 and Tyr77-Leu33 (Table 2, Figure 7). The intramolecular hydrogen bonds of the monomers remained unchanged in the L33S protein. Besides two intermolecular hydrogen bonds that are available in the WT sHSP, the L33S

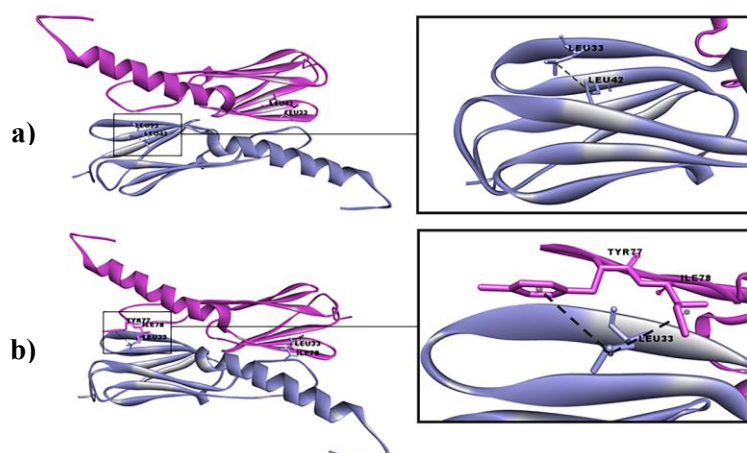
mutation formed an additional one between the nitrogen atom of Ile78 and the oxygen atom of Ser33. Moreover, the decrease in the hydrogen bond distance was remarkable, particularly those involved in intermolecular interactions (Table 2). On the other hand, substituting tyrosine with the highly hydrophobic phenylalanine at position 34 by Y34F mutation did not result in any apparent changes in the predicted intramolecular hydrogen and intramolecular hydrophobic interactions (Figure 8). However, it caused alterations in the distances between these bonds, as indicated in Table 3.

Table 2. Intermolecular and intramolecular bond analysis of L33S mutant sHSP as compared with the WT sHSP

Hydrogen Bond in WT	Distance	Hydrophobic interactions in WT	Distance	Hydrogen Bond in L33S	Distance
Intramolecular Interactions			Intramolecular Interactions		
B:LEU33:CA - B:VAL41:O	3,3591	A:LEU33 - A:LEU42	4,6659	B:SER33:CA - B:VAL41:O	3,1639
A:LEU33:CA - A:VAL41:O	3,35931	B:LEU33 - B:LEU42	4,6663	A:SER33:CA - A:VAL41:O	3,1639
Intermolecular Interactions			Intermolecular Interactions		
B:LEU33:N - A:ILE78:O	3,0712	A:LEU33 - B:ILE78	5,1210	B:SER33:N - A:ILE78:O	2,8393
B:ILE78:N - A:LEU33:O	3,0231	A:ILE78 - B:LEU33	4,6994	B:ILE78:N - A:SER33:O	2,6742
		A:TYR77 - B:LEU33	5,4574	A:ILE78:N - B:SER33:O	2,0301

Table 3. Intramolecular bond analysis of Y34F mutant sHSP as compared with the WT sHSP

Hydrogen Bond in WT	Distance	Hydrophobic interactions in WT	Distance	Hydrogen Bond in Y34F	Distance	Hydrophobic interactions in Y34F	Distance
Intramolecular Interactions				Intramolecular Interactions			
B:TYR34:N- B:VAL41:O	3,12704	A:TYR34- A:VAL41	4,03417	B:PHE34:N-B:VAL41:O	3,0023	B:VAL41:CB- B:PHE34	3,8605
B:VAL41:N- B:TYR34:O	2,98035	B:TYR34- B:VAL41	4,03407	B:VAL41:N-B:PHE34:O	3,0042	A:VAL41:CB- A:PHE34	3,8610
A:TYR34:N- A:VAL41:O	3,12661			A:PHE34:N-A:VAL41:O	3,0017		
A:VAL41:N- A:TYR34:O	2,97915			A:VAL41:N- A:PHE34:O	3,0049		

**Figure 7.** Intra (a) and intermolecular (b) hydrophobic bonds of *Tpv* HSP 14.3 WT at residue Leu33. Pink indicates the one monomer and blue indicates the partner monomer.

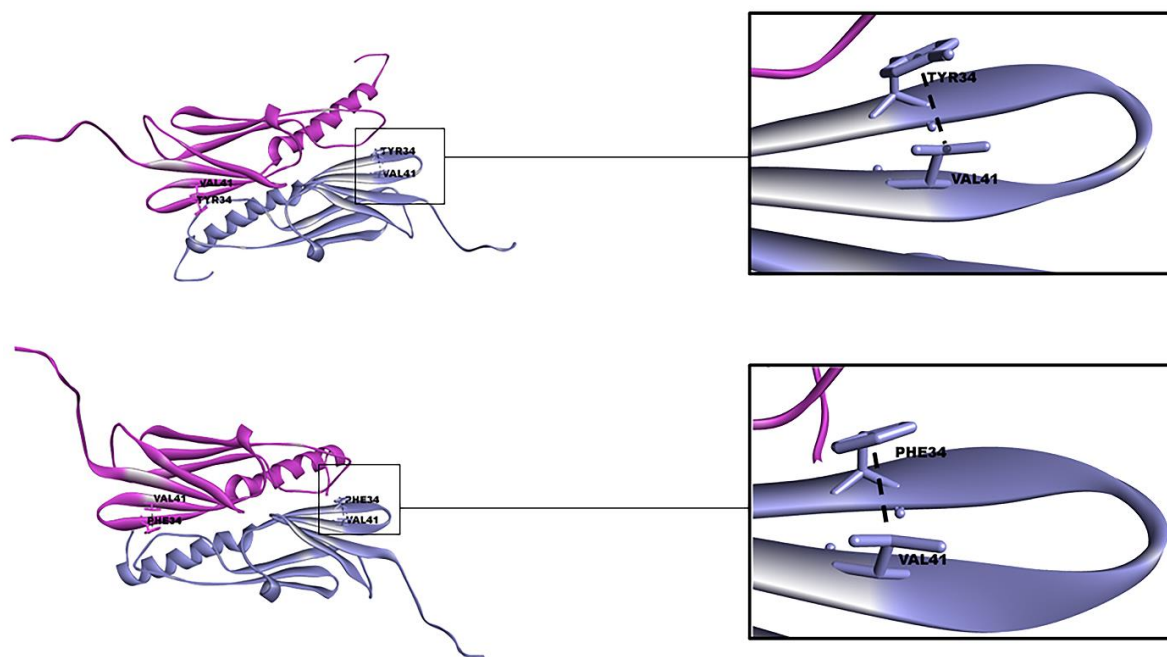


Figure 8. Intramolecular hydrophobic bonds of *Tpv* HSP 14.3 WT (a) and Y34F mutant (b) at residue 34. Pink indicates the one monomer and blue indicates the partner monomer.

3.5 Thermodynamic Stability Analysis of *Tpv* HSP 14.3 Mutants

The stability of proteins is a critical feature that affects their proper functioning, activity, and regulation. Protein thermodynamic stability is quantified by ΔG , which is equal to the difference between the free energy of folded and unfolded states [24]. In order to predict the thermodynamic stability of the mutant sHSPs, we used the MUpro web server. When the relative stability change ($\Delta\Delta G$), which is the difference between the free energy of wild type protein and mutant proteins, is positive, it indicates that the mutation increases stability and vice versa. The method relies on a confidence score between -1 to 1. A score less

than 0 is attributed to the reduced stability after mutation [23]. According to the MUpro analysis, the thermodynamic stability of *Tpv* HSP 14.3 ACD mutants decreased. The L33S mutant ($\Delta\Delta G = -2.203$) was apparently less stable as compared to the Y34F mutant ($\Delta\Delta G = -0.41$).

4 DISCUSSION

Identifying residues crucial for the ACD dimerization has been documented so far through crystallographic analysis of the sHSP structures from a limited number of species [11, 25–28]. Also, this issue has remained poorly explored experimentally by mutagenesis in archaeal sHSPs. Our research

has focused on two putative interface residues, L33 and Y34, located on the $\beta 2$ strand of the *Tpv* HSP 14.3, which is involved in ACD dimerization *via* strand exchange, to investigate the functional and structural consequences of these targeted amino acid substitutions.

Our results indicated that *Tpv* HSP 14.3 WT and its two mutant variants, were unaffected from exposure to high temperatures up to 70°C, as deduced by SDS-PAGE analysis. Above this temperature, although there has been a detectable decrease in the solubility of the L33S mutant sHSP relative to WT sHSP, a slight decrease in solubilization of the Y34F mutant protein was observed. Further assessment of the thermodynamic stability by MUpro analysis also suggested that the decline in the thermodynamic stability of the sHSP protein was more pronounced with the L33 to S exchange than with the Y34 to F substitution. It was observed that each hydrogen bond distance in L33S changed remarkably as compared to the WT sHSP. As previously reported, a change in hydrogen bond distance may cause loss of thermodynamic stability as well as aberrant folding and aggregation of the proteins [29, 30]. In addition, the loss of intermolecular hydrophobic interactions between the Leu33 on the $\beta 2$ strand and Tyr77 and Ile78 on the $\beta 6$ loop of the ACD dimer should also be critical for the reduced stability of the L33S mutant. Similarly, the Leu33-

Tyr77 hydrophobic interaction in *Tpv* HSP 14.3 is equivalent to Ile47-Tyr96 inter-subunit contact in the ACD of the MjHSP16.5 (from *Methanococcus jannaschii*) and analysis of its crystal structure suggested that this interaction can be involved in the stabilization of the MjHSP16.5 structure [25]. Thus, our result also complements the previous reports that proposed the hydrophobic interactions as the critical factors contributing to the thermal stability of thermophilic proteins [31].

The Y34F mutation did not alter hydrophobic interactions, and the change in the bond distances was not significant in the Y34F mutant relative to the WT sHSP, as well. Therefore, Y34 replacement by more hydrophobic F did not produce a dramatic effect on the solubility as well as the stability of the sHSP protein. Also, it is likely that Y34 to F substitution produced newly exposed hydrophobic surfaces on ACD, which could act as substrate binding sites. At the high chaperone concentrations (*i.e.*, 1:500 w/w substrate/sHSP ratio), both L33S and Y34F mutants performed 9 to 10% higher protection of the phCS activity as compared to positive control. However, the L33S sHSP was less efficient than the Y34F sHSP for protection of ADH at 1:90 w/w substrate/chaperone ratio and protection of the phCS at lower concentrations (*i.e.*, substrate/chaperone ratio of 1:147) from heat inactivation. The greater ability of Y34F compared with the L33S to

protect these two substrates can be hypothesized to arise from its increased hydrophobicity that may contribute to forming a hydrophobic surface. This result is compatible with previously published data suggesting that at higher temperatures, elevated chaperone activity of the sHSPs is mainly due to exposure of their buried hydrophobic patches which can readily capture aggregation-prone substrates [28, 32–34]. In parallel to our findings in *Drosophila melanogaster* Hsp27 and human CRYAB, mutations that involve substitutions by hydrophobic residues were found to be associated with altered surface properties and increased the chaperone activity [35, 36]. In mouse CRYAB, hydrophobicity at position 68 (M68) (which is equivalent to the L33 of *Tpv* HSP 14.3) was found to be important for chaperone function. Increasing hydrophobicity by replacing methionine with highly hydrophobic amino acids (Ile or Val) improved the chaperone activity, while decreasing hydrophobicity with polar residue substitution (Thr) reduced its activity [37].

In conclusion, this study sheds light on the dual importance of hydrophobic interactions at the dimer interface of *Tpv* HSP 14.3 for maintaining the structural/thermodynamic stability and effectiveness of the chaperone function. Our findings can contribute not only to understanding the molecular mechanisms behind sHSPs action but also to the affords for

developing therapeutic strategies that target the diseases that result from protein misfolding and aggregation (e.g., cataract, Alzheimer's Disease, Parkinson's Disease)[1, 38–40].

5 ACKNOWLEDGEMENTS

The authors acknowledge METU-BAP for partially supporting this project with grants (TEZ-D-108-2020-10187).

6 AUTHOR CONTRIBUTIONS

Hypothesis: S.K., ; Design: S.K., S.Z.; Literature review: S.K., S.Z.; Data Collection: S.K., S.Z., A.R. ; Analysis and/or interpretation: S.K., S.Z.; Manuscript writing: S.K., S.Z.

7 CONFLICT OF INTEREST

The Authors declare that there is no conflict of interest.

8 REFERENCES

- [1] Hu C et al. Heat shock proteins: Biological functions, pathological roles, and therapeutic opportunities. *MedComm*, 2022;3(3):1–39. DOI:10.1002/mco2.161
- [2] Macario a J et al. Stress genes and proteins in the archaea. *Microbiology and molecular biology reviews* : MMBR, 1999;63(4):923–967. DOI: 10.1128/MMBR.63.4.923-967.1999
- [3] Haslbeck M, Vierling E. A First Line of Stress Defense: Small Heat Shock Proteins and Their Function in Protein Homeostasis. *Journal of Molecular Biology*, 2015;427(7):1537–1548. DOI:10.1016/j.jmb.2015.02.002

- [4] Tedesco B et al. Insights on Human Small Heat Shock Proteins and Their Alterations in Diseases. *Frontiers in Molecular Biosciences*, 2022;9:1–27. DOI:10.3389/fmolb.2022.842149
- [5] Roy M, Bhakta K, Ghosh A. Minimal Yet Powerful: The Role of Archaeal Small Heat Shock Proteins in Maintaining Protein Homeostasis. *Frontiers in Molecular Biosciences*, 2022;9:1–9. DOI:10.3389/fmolb.2022.832160
- [6] Haslbeck M, Weinkauff S, Buchner J. Small heat shock proteins: Simplicity meets complexity. *Journal of Biological Chemistry*, 2019;294:2121–2132. DOI:10.1074/jbc.REV118.002809
- [7] Reinle K, Mogk A, Bukau B. The Diverse Functions of Small Heat Shock Proteins in the Proteostasis Network. *Journal of Molecular Biology*, 2021;434(1):167–157. DOI:10.1016/j.jmb.2021.167157
- [8] Mogk A, Ruger-herreros C, Bukau B. Cellular Functions and Mechanisms of Action of Small Heat Shock Proteins. *Annual Review of Microbiology*, 2019;73:89–110. DOI:10.1146/annurev-micro-020518-115515
- [9] Hayashi J, Carver JA. The multifaceted nature of α B-crystallin. *Cell Stress and Chaperones*, 2020;25(4):639–654. DOI:10.1007/s12192-020-01098-w
- [10] Mogk A, Bukau B. Role of sHsps in organizing cytosolic protein aggregation and disaggregation. *Cell Stress and Chaperones*, 2017;22(4):493–502. DOI:10.1007/s12192-017-0762-4
- [11] Hilario E et al. Crystal structures of xanthomonas small heat shock protein provide a structural basis for an active molecular chaperone oligomer. *Journal of Molecular Biology*, 2011;408(1):74–86. DOI:10.1007/s12192-017-0762-410.1016/j.jmb.2011.02.004
- [12] Obuchowski I, Karaś P, Liberek K. The Small Ones Matter—sHsps in the Bacterial Chaperone Network. *Frontiers in Molecular Biosciences*, 2021;8:1–7. DOI:10.3389/fmolb.2021.666893
- [13] Hilton GR et al. C-terminal interactions mediate the quaternary dynamics of α B-crystallin. *Philosophical Transactions of the Royal Society B: Biological Sciences*, 2013;368(1617):1–13. DOI:10.1098/rstb.2011.0405
- [14] Clark a. R et al. Crystal structure of R120G disease mutant of human α B-crystallin domain dimer shows closure of a groove. *Journal of Molecular Biology*, 2011;408(1):118–134. DOI:10.1016/j.jmb.2011.02.020
- [15] Kim M V et al. Structure and properties of K141E mutant of small heat shock protein HSP22 (HspB8, H11) that is expressed in human neuromuscular disorders. *Archives of Biochemistry and Biophysics*, 2006;454(1):32–41. DOI:10.1016/j.abb.2006.07.014
- [16] Litt M et al. Autosomal dominant congenital cataract associated with a missense mutation in the human alpha crystallin gene CRYAA. *Human Molecular Genetics*, 1998;7(3):471–474. DOI:10.1093/hmg/7.3.471
- [17] Vicart P et al. A missense mutation in the alphaB-crystallin chaperone gene causes a desmin-

- related myopathy. *Nature Genetics*, 1998;20(1):92–95. DOI:10.1038/1765
- [18] Kasakov AS et al. Effect of mutations in the β 5- β 7 loop on the structure and properties of human small heat shock protein HSP22 (HspB8, H11). *FEBS Journal*, 2007;274:5628–5642. DOI:10.1111/j.1742-4658.2007.06086.x
- [19] Quinlan RA et al. Changes in the quaternary structure and function of MjHSP16.5 attributable to deletion of the IXI motif and introduction of the substitution, R107G, in the α -crystallin domain. *Philosophical Transactions of the Royal Society of London. Series B, Biological Sciences*, 2013;368(1617):20120327. DOI:10.1098/rstb.2012.0327
- [20] Kocabiyik S, Aygar S. Improvement of protein stability and enzyme recovery under stress conditions by using a small HSP (tpv-HSP 14.3) from *Thermoplasma volcanium*. *Process Biochemistry*, 2012;47(11):1676–1683. DOI:10.1016/j.procbio.2011.11.014
- [21] Kagi JH, Vallee BL. The role of zinc in alcohol dehydrogenase. V. The effect of metal-binding agents on the structure of the yeast alcohol dehydrogenase molecule. *The Journal of Biological Chemistry*, 1960;235:3188–3192. PMID: 13750715.
- [22] Waterhouse AM et al. Jalview Version 2-A multiple sequence alignment editor and analysis workbench. *Bioinformatics*, 2009;25(9):1189–1191. DOI: 10.1093/bioinformatics/btp033
- [23] Cheng J, Randall A, Baldi P. Prediction of protein stability changes for single-site mutations using support vector machines. *Proteins: Structure, Function and Genetics*, 2006;62(4):1125–1132. DOI: 10.1002/prot.20810
- [24] Bigman LS, Levy Y. Entropic Contributions to Protein Stability. *Israel Journal of Chemistry*, 2020;60(7):705–712. DOI: 10.1002/ijch.202000032
- [25] Kim KK, Kim R, Kim SH. Crystal structure of a small heat-shock protein. *Nature*, 1998;394(6693):595–599. DOI:10.1038/29106
- [26] Liu L et al. Active-State Structures of a Small Heat-Shock Protein Revealed a Molecular Switch for Chaperone Function. *Structure*. 2015;23(11):2066–2075. <http://dx.doi.org/10.1016/j.str.2015.08.015>. DOI:10.1016/j.str.2015.08.015
- [27] Hanazono Y et al. Structural Studies on the Oligomeric Transition of a Small Heat Shock Protein, StHsp14.0. *Journal of Molecular Biology*, 2012;422(1):100–108. DOI:10.1016/j.jmb.2012.05.017
- [28] van Montfort RL et al. Crystal structure and assembly of a eukaryotic small heat shock protein. *Nature Structural Biology*, 2001;8(12):1025–1030. DOI:10.1038/nsb722
- [29] Chen J, Shen B. Computational Analysis of Amino Acid Mutation: A Proteome Wide Perspective. *Current Proteomics*, 2009;6(4):228–234. DOI: 10.2174/157016409789973734
- [30] Doss CGP, NagaSundaram N. Investigating the structural impacts of I64T and P311S mutations in APE1-DNA complex: A molecular dynamics approach. *PLoS ONE*,

2012;7(2):1–11.

DOI:10.1371/journal.pone.0031677

[31] Goldstein RA. Amino-acid interactions in psychrophiles, mesophiles, thermophiles, and hyperthermophiles: Insights from the quasi-chemical approximation. *Protein Science*, 2007;16(9):1887–1895.

DOI:10.1110/ps.072947007

[32] Das KP, Surewicz WK. Temperature-induced exposure of hydrophobic surfaces and its effect on the chaperone activity of α -crystallin. *FEBS Letters*, 1995;369:321–325. DOI: 10.1016/0014-5793(95)00775-5

[33] Kim R et al. On the mechanism of chaperone activity of the small heat-shock protein of *Methanococcus jannaschii*. *Proceedings of the National Academy of Sciences of the United States of America*, 2003;100(8):8151–8155. DOI: 10.1073/pnas.1032940100

[34] Bova MP, Huang Q, Ding L, Horwitz J. Subunit exchange, conformational stability, and chaperone-like function of the small heat shock protein 16.5 from *Methanococcus jannaschii*. *Journal of Biological Chemistry*, 2002;277(41):38468–38475. DOI: 10.1074/jbc.M205594200

[35] Moutaoufik MT et al. Oligomerization and chaperone-like activity of *Drosophila melanogaster* small heat shock protein DmHsp27 and three arginine mutants in the alpha-crystallin

domain. *Cell Stress and Chaperones*, 2017;22:455–466. DOI:10.1007/s12192-016-0748-7

[36] Santhoshkumar P, Sharma KK. Conserved F84 and P86 residues in α B-crystallin are essential to effectively prevent the aggregation of substrate proteins. *Protein Science*, 2006;15:2488–2498. DOI: 10.1110/ps.062338206

[37] Shroff NP, Bera S, Cherian-Shaw M, Abraham EC. Substituted hydrophobic and hydrophilic residues at methionine-68 influence the chaperone-like function of α B-crystallin. *Molecular and Cellular Biochemistry*, 2001;220:127–133. DOI: 10.1023/A:1010834107809

[38] Zabci S. Therapeutic importance of small heat shock proteins and their interactions with other proteins In: Arıcı Y, Hancı H (ed). *Multidisciplinary Approach to Basic and Clinical Science*. Ankara:IKSAD International Publishing House; 2023:61-77.[ISBN: 978-625-367-203-4]

<https://iksadyayinevi.com/home/multidisciplinary-approach-to-basic-and-clinical-science/>

[39] Mymrikov E V., Seit-Nebi AS, Gusev NB. Large potentials of small heat shock Proteins. *Physiological Reviews*, 2011;91(4):1123–1159. DOI:10.1152/physrev.00023.2010

[40] Muranova LK et al. Small Heat Shock Proteins and Human Neurodegenerative Diseases. *Biochemistry*, 2019;84(11):1256–1267. DOI: 10.1134/S000629791911004X